

# Reassessment of Basin Evolution Premise of Bhima Basin in Light of High Resolution Aeromagnetic Data

M Sridhar\*, V Ramesh Babu, J K Patnaik, Rakesh Mohan, R Mamallan, B Saravanan

Atomic Minerals Directorate for Exploration and Research, Hyderabad, Telangana, India

## ABSTRACT

The tectonic signatures for the extensional basin evolution are generally not well developed and it is relatively difficult to reconstruct, particularly when affected by a strong deformation associated with subsequent compressional tectonics. In the present study, an attempt has been made to map structural elements buried beneath younger cover in Bhima basin, by using aeromagnetic data. The magnetic data indicates that around Malla Buzurg, a NE-SW trending fault affects the Gogi Fault and swerves it towards southwest Kalakeri. Bhima basin has possibly evolved over a failed E-W trending rift zone, surmised as reactivation post sedimentation of Bagalkot Group. Later the NE-SW shear couple bounding the geometry to a lozenge shape with long axis along NE-SW, probably defined the basin boundaries and the NW-SE trending dextral strike slip faults have defined the present day basin configuration.

**Keywords:** Bhima basin; Aeromagnetic data; Basin configuration; Tectonic evolution; Rift basin

## INTRODUCTION

The Proterozoic platform sequences of Peninsular India preserve signatures of widely divergent lithospheric processes and workers have suggested the sedimentation within the Purana basins as the ambit of eperic sea framework. However, recent studies have put forward rift and foreland models for the initiations of many of the Purana basins [1]. In contrast to the traditional evolutionary models of Purana basins, Neo-Proterozoic Bhima basin in the northern fringe of Eastern Dharwar craton exposing sediments of Bhima Group in a NE-SW trending en echelon pattern presents a unique setting befitting tectonic control as suggested by many workers [2-5]. Sedimentological studies of these sediments by Akhtar et al. [2], and Mudholkar et al. [6], explicitly surmise that the Bhima sediments represent platform deposits of shallow marine, near shore environments. Structural mapping and geological studies of the Bhima basin suggest that these sediments were subjected to buckling or compressional deformation [7]. Ramakrishna et al. [8], based on the gravity anomaly of 10 mGal to 15 mGal has estimated sediment thickness of approximately 1.5 km and inferred that the Bhima sediments have not witnessed any major faulting or tectonic movement. This is refuted by Kale et al. [3], who put forward a pull-apart model for the formation of the basin triggered by NW-SE shear couple based on field evidences such as clastic dykes, slump structures, intra-formational breccia

and folding along with remote sensing studies. They suggested that few faults have reactivated during sedimentation and possibly have played significant role in sedimentation within the basin [4]. Later, the pull-apart model was modified by Jayaprakash et al. [5], who suggested that the basin is formed by pull-apart with sinistral movement along a major curvilinear strike-slip fault trending NE-SW direction. These models laid by past workers are based on limited field evidences and inadequate regional geophysical inputs and hence are not tenable. Further, due to paucity of comprehensive geophysical data left with several disagreements regarding the tectonic evolution of Bhima basin.

In order to understand and constrain tectonic evolutions of concealed and meagerly exposed terrains particularly of Precambrian age, over the past decades high-resolution aeromagnetic data has been extensively employed [9-11]. Resolving complexities and overprinting events in geological evolutions of these terrains, a systematic approach with sound reasoning based on reliable data would grant insight into tectonic processes. The study based on aeromagnetic data for sedimentary basins has increased with the development of high-resolution surveys and filtering techniques [12-14], allowing improvement of the structural models of sedimentary basins and margins by locating buried intra-basinal faults [11,15-18]. In line with these studies, our focus was on the interpretation of aeromagnetic data of the Bhima Basin to unravel the structure, basin-fill architecture

**Correspondence to:** Sridhar Muthyala, Atomic Minerals Directorate for Exploration and Research, Hyderabad, Telangana, India, Tel: +919493410682; E-mail: msridhar.research@gmail.com

**Received:** 17-Nov-2023, Manuscript No. JGG-23-28053; **Editor assigned:** 20-Nov-2023, PreQC. No. JGG-23-28053 (PQ); **Reviewed:** 04-Dec-2023, QC. No. JGG-23-28053; **Revised:** 11-Dec-2023, Manuscript No. JGG-23-28053 (R); **Published:** 18-Dec-2023, DOI: 10.35248/2381-8719.23.12.1164.

**Citation:** Sridhar M, Babu VR, Patnaik JK, Mohan R, Mamallan R, Saravanan B (2023) Reassessment of Basin Evolution Premise of Bhima Basin in Light of High Resolution Aeromagnetic Data. J Geol Geophys. 12:1164.

**Copyright:** © 2023 Sridhar M, et al. This is an open-access article distributed under the terms of the Creative Commons Attribution License, which permits unrestricted use, distribution, and reproduction in any medium, provided the original author and source are credited.

and the basement configuration. This led to understanding the deformation history and its role in basin evolution with the aim of placing the crustal scale events into a regional and global context.

## Geology of the area

The Dharwar Craton of Peninsular India consists of two parts; (A) The older Western Dharwar Craton (WDC; 3.3–2.7 Ga), and (B) The younger Eastern Dharwar Craton (EDC; 3.0–2.5 Ga) [19]. The WDC is dominated by volcano-sedimentary greenstone belts and TTG granitoids, ranging in age from 3.3 to 2.7 Ga. The EDC is predominantly made of Neoproterozoic granites and sub-ordinate volcanic-dominated linear greenstone belts of limited dimensions [20]. The EDC comprises Dharwar Batholith (dominantly granitic), greenstone belts, intrusive volcanics, and middle Proterozoic to more recent sedimentary basins (Figure 1) [21,22].

The Mesoproterozoic sequence of Bhima group shows unconformable as well as tectonic contact, mainly with the Neoproterozoic granitoid basement and to a lesser extent with greenstone belts. Peshwa et al. [23], have pointed out that the Bhima sediments display unconformable relationships with the basement along the N-S to NNE-SSW trending rectilinear eastern margins, whereas the E-W to WNW-ESE trending rectilinear southern boundaries are all of faulted nature. The flat lying sedimentary formations of the Bhima Group are exposed as an array of narrow east-west trending, sigmoid strips, arranged in an en echelon pattern and reach a maximum thickness of 270 m [24]. These sedimentary rocks comprise an alternating sequence of clastic and carbonate components, with oligomictic conglomerate (maximum thickness 2 m) at the base, followed by sandstone, shale and limestone [4,24]. The Northern and Western parts of Bhima basin is covered by Deccan Trap basalts of unknown thickness. Different classifications are proposed for the sedimentary succession, Mishra et al. [24], divided the Bhima sediments into two subgroups separated by a paraconformity, the lower Sedam subgroup composed of Rabanpalli and Shahabad formations and upper subgroup called Andola sub-group Harwal, Katamdevarahalli and Halkal formations. Later, based on interpretations of Landsat imageries and air-photos Kale et al. [4], proposed a two-fold classification, the lower Rabanpalli formation consisting of conglomerate, arenite and shale and the upper Shahabad formation dominated by limestones. Jayaprakash et al. [5], reiterated the five-fold stratigraphic classification of the Bhima group with aggregate thickness of about 300 m approximately. The lowermost Rabanpalli formation is represented by coarse rudaceous to fine argillaceous clastics and overlying Shahabad formation is essentially a chemical precipitate. The upper Halkal, Katamdevarahalli and Harwal formations are essentially made up of litho-components viz. shale, limestone and shale respectively. The depositional history proposed by different works vary from beaches or intertidal deltaic zone grading laterally into a relatively deeper tidal flat or subtidal environment, shallow-marine environment [2,4], with pulsating sea-level changes.

There is no pronounced evidence that Bhima group is affected by any major event of structural upheaval on a regional scale. The broad sub-horizontal disposition sediments of Bhima group are mostly horizontal and are considered to be undisturbed or least deformed. Kale et al. [4], opined that many of the folds seen in the basin are the products of slumping and not related to diastrophism; sub-horizontal nature of the beds are due

to depositional dips. Structurally, the basin is transected by prominent E-W and NW-SE trending faults besides a number of smaller N-S and NE-SW trending faults. Jayaprakash et al. [5], reported development of stylolites within Bhima sediments particularly carbonate strata, and these structures are known to form in response to tectonic compression [25]. Many of the larger faults qualify not only as faulted boundaries but also as boundary faults of this basin, defining the structural boundary of the basin. These faults exhibit intense brecciation and locally intense tight, at places isoclinal and recumbent folding observed along narrow zones in the vicinity of the faults associated with the Bhima Basin [4].

## MATERIALS AND METHODS

### High resolution heliborne magnetic data acquisition and processing

The heliborne survey operations were carried out in three phases and acquired 47000 line km of high-resolution magnetic data by employing geometrics optically pumped cesium magnetometer towed below the helicopter. The data is acquired at 10 Hz sampling rate with a sample spaced at ~2.5 m along transverse lines oriented in the N-S direction and spaced at 200 m and a long tie-line oriented in the E-W direction and spaced at 5000 m over Bhima basin (Figure 1).

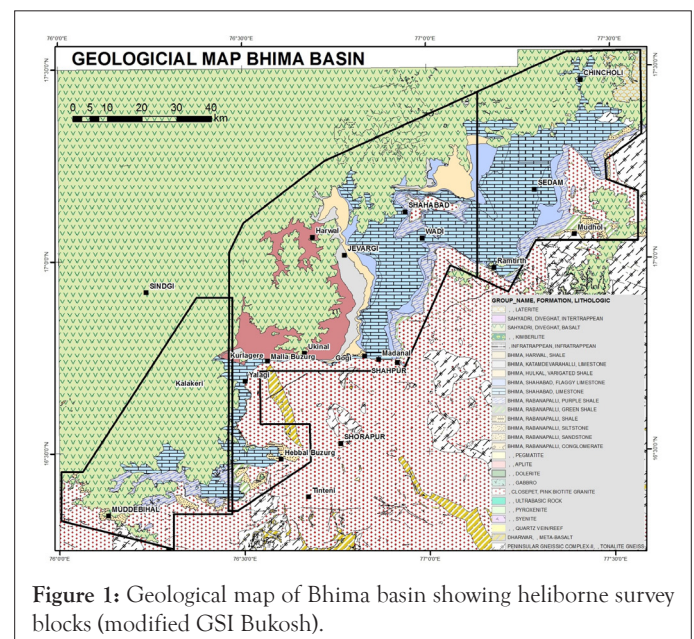


Figure 1: Geological map of Bhima basin showing heliborne survey blocks (modified GSI Bukosh).

The acquired magnetic data is processed by applying correction for diurnal variations by using the digitally recorded ground base station magnetic values. Heading error and lag corrections are applied by utilising coefficients obtained from heading and lag test flight data. Tie line levelling was carried out by adjusting intersection points along traverse lines. A micro-levelling procedure was applied to remove persistent low-amplitude components of flight-line-direction-related noise in the data. The magnetic data were corrected for the International Geomagnetic Reference Field (IGRF) by subtracting the IGRF model values at each point in the survey, and a constant value (42345 nT) was added to each data point. The corrected magnetic data were interpolated between survey lines using a random point gridding method to yield x-y grid values for a standard grid cell size of approximately 50 m at the mapping scale. A minimum curvature algorithm [26], was used to interpolate values onto a rectangular





The total magnetic intensity image, first vertical derivative and the tilt derivative grid images were utilized to infer the magnetic linears and breaks. The frequency plot of the linear azimuths suggests that the majority of the trends occur between NW-SE to SW-NE, and the dominant is along NW-SE, followed by E-W and SW-NE directions. Accordingly the linears are classified into three categories and the regional trends are demarcated (Figure 3). Based on the dislocation and abutment of magnetic linear,

the sequence of trends is inferred i.e., the oldest E-W trends are dislocated by NE-SW and the youngest trends are NW-SE directions disrupts the predecessors. The upward continuation of the aeromagnetic data indicates that these NW-SE and few E-W directions are prominent even at 1000 m above terrain, suggesting that they are of deep-seated origin and probably faults rather than dykes (Figure 4).

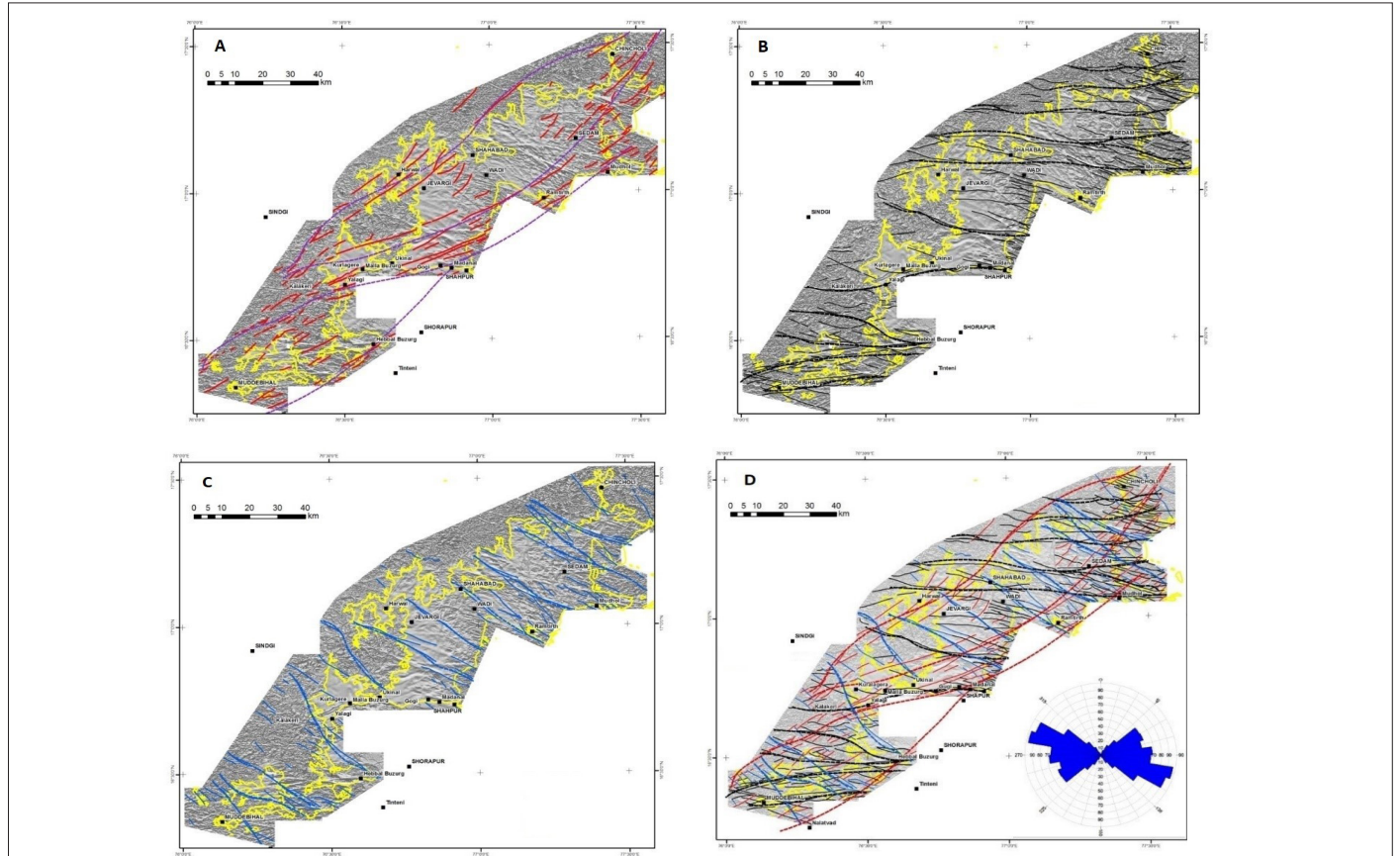


**Figure 3:** RTP-FVD grid image with basin outline (yellow) showing magnetic breaks and linears. A) NE-SW, B) E-W, C) NW-SE and D) Combined. Note: ( — ) NW-SE (lineament), ( - - - )NW-SE, ( ——— ) E-W (lineament), ( - - - - ) E-W, ( ——— ) N-S (lineaments), ( ——— ) NE-SW (lineaments), ( — - - ) NE-SW, ( □ ) Bhima sediments, ( ■ ) City.

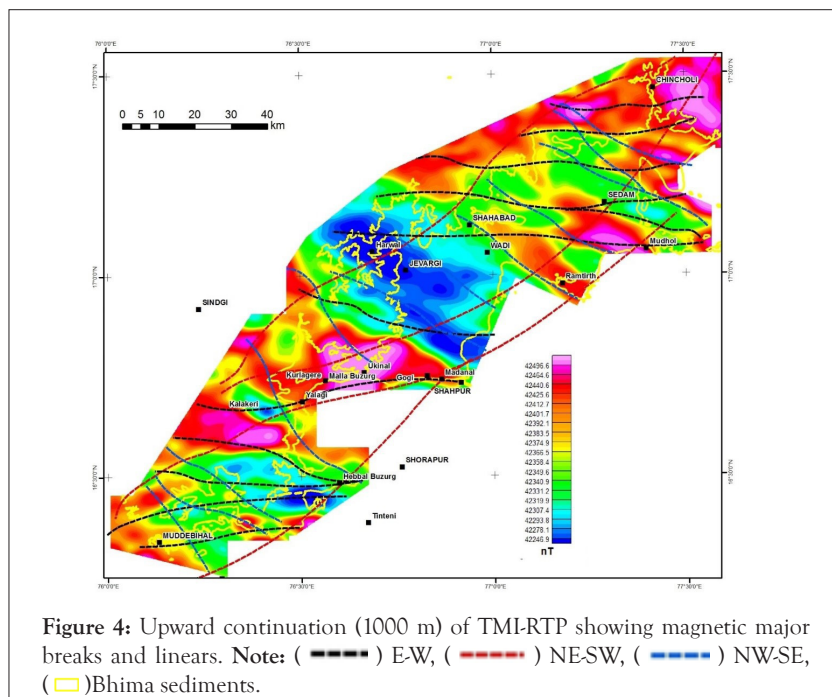


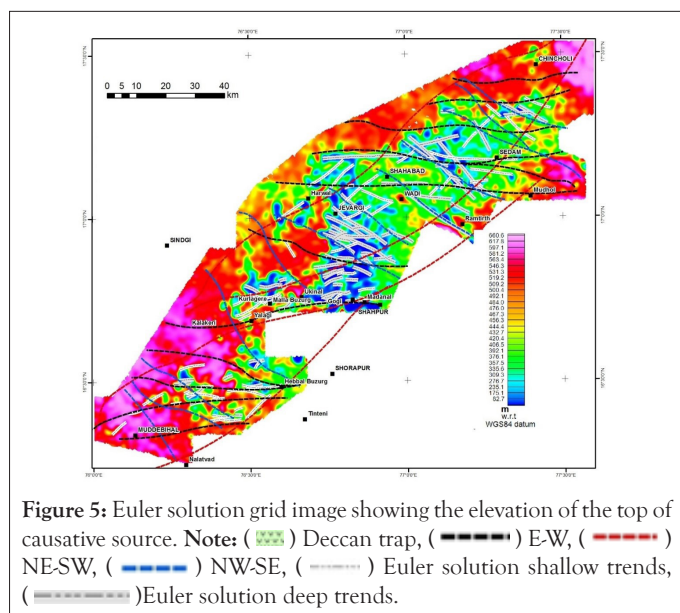
**Figure 4:** Upward continuation (1000 m) of TMI-RTP showing magnetic major breaks and linears. Note: ( - - - - ) E-W, ( - - - - ) NE-SW, ( - - - - ) NW-SE, ( □ )Bhima sediments.

## RESULTS

### Quantitative interpretation

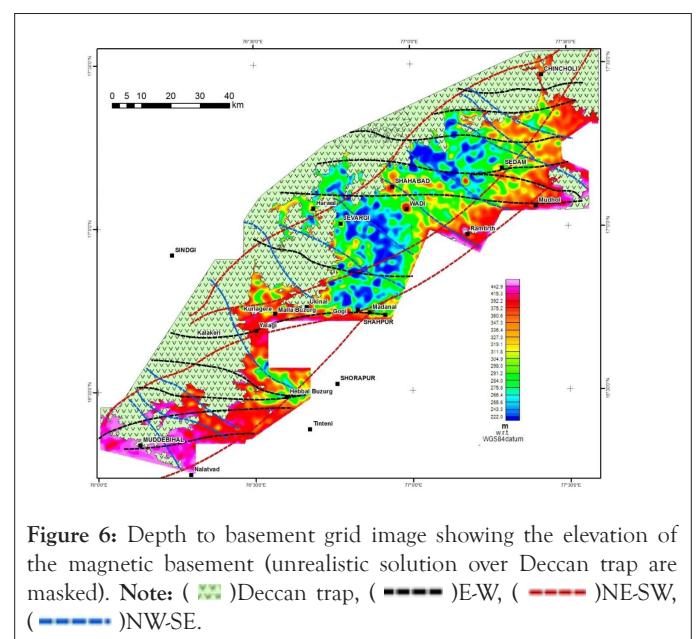
In order to compute the values associated with the inferred geological features, few quantitative methods which are routinely used are employed.

**Depth estimates by Euler deconvolution:** Euler algorithm utilizes the spatial derivative of the magnetic field for the estimation of the depth to the top of the magnetic structure. The conventional approach uses Euler equation [31], and in the present case the solutions are estimated using both the conventional Euler equation and the rotational constraint equation from extended Euler [32]. This approach solves both equations jointly (extended Euler) to give distance, depth, dip, and susceptibility, assuming there is no remnant magnetization. Later, the solution are validated by estimates of conventional Euler Deconvolution and the relative difference in depths by the two estimates is less than the given maximum percentage error, the solution is retained; rejected otherwise. The solution for contact with Structural Index (SI) of zero and structural index of one for dyke is calculated. This generates a spray of solutions around the real solution due to multiple passes with different window lengths and is hence clustered (grouped) into single, average solution. In view of the preponderance of dyke-like sources that is evident in the map, solution of structural index of 1 are plotted on the map, indicates that the solutions are lined up along the structure. Deeper sources are seen between Gogi-Jevargi and Wadi-Sedam, absence of shallow magnetic sources is quite evident which further extends towards west, presumably the basin could deepen further below the Traps. The solutions are classified as shallow (<300 m) and deeper (>300 m) and the most obvious alignments of interpreted sources were then drawn as lines, corresponding mostly to the dykes and faults in the original data. The ability of the method to pick out linear structures leads often to the revelation of conjugate faults sets in hard rock areas, even where it is not evident at first sight in magnetic maps. The marked linears suggest that the NW-SE trending faults are deep seated and the NE-SW trends are mostly shallow. Jayaprakash et al. [5], opined that the NW-SE trending faults are deep seated and few of the E-W faults indicate variable depths i.e. they are shallow source towards the east and deeper towards the west (Figure 5).



**Depth to basement:** Dykes in general provide clear magnetic anomalies; estimations of depths to the causative dyke bodies from their anomalies can be used to estimate the thickness of any overlying cover in many survey locations. However, to know the depth of the Bhima basin (basement configuration) in the present case, the presence of (some) dykes of post-sediment age, implies that this may be of limited application. Majority dykes predate the Bhima sediments and usually terminate at the unconformity between the Archean basement and the Neoproterozoic basin, these could then be used to estimate the depth of the basin. Such basin depth is thought not to exceed about 300 m from the maximum measured thickness of stratigraphic units within it.

Magnetic depth estimation by Werner Deconvolution [33], which is a profile-based automated technique was used to generate a Depth to magnetic Basement (DTB) model over the Bhima basin. This technique operates on a segment of the anomaly profile referred to as a window, and estimates a theoretical depth estimate to the top of the body and the window moves along the profile. By varying the window size between 500 m and 5000 m with an increment of 100 m, solution sets are created. The structural index of '1' for dyke type body and structural index (0) for contact were assigned for depth estimates. Each solution set was clustered in order to determine an average "true solution" for the depth to basement independent of the solution windows defined above. In this technique, the solutions close to the boundary of the grid are unrealistic; hence the outer 1000 m of data should be used with low confidence. The estimates are filtered by removing spurious/spikes solution and the solutions are presented as a grid of basement elevation with respect to WGS84 datum (Figure 6). The estimates in the west side are masked, as the estimates made over the Deccan Traps are not reliable due to their interference with magnetic signal. The basement elevation grid ranges from approximately 650 m to 149 m respectively to WGS84 datum. The grid generated from Extended Euler solutions corroborate well with the DTB grid generated by Werner Deconvolution, however the later is more consistent with the outcropping basement rocks. The grid image indicate two major depressions (i) trending from Gogi towards NE and swerve NW towards Jevargi and Harwal (ii) linear NW-SE trending depression north of Shahabad. The depression north of Shahabad continues towards northwest and further it is covered by Deccan Trap, apparently it is inferred that the depression continues beneath the trap cover. Paleocurrent studies by Akhtar et al. [2], suggested that the direction of current moving due NW, which substantiated with the inference of basin deepening towards NW.





The high resolution digital elevation data acquired simultaneously with the magnetic data is utilized for generating the DEM grid image showing elevation range of 363 m to 665 m. By subtracting the Basement Topography Grid (DTB) from the surface topography (DEM) the apparent thickness of sediments is estimated as shown in Figure 7. The maximum sedimentary thickness estimated in the basin is 274 m, which concur with the suggested stratigraphic thickness of 270 m [24], and 300 m [5]. All the non-magnetic sediments and metasediments above the magnetic basement are accounted for while estimating thickness of Bhima sediment.

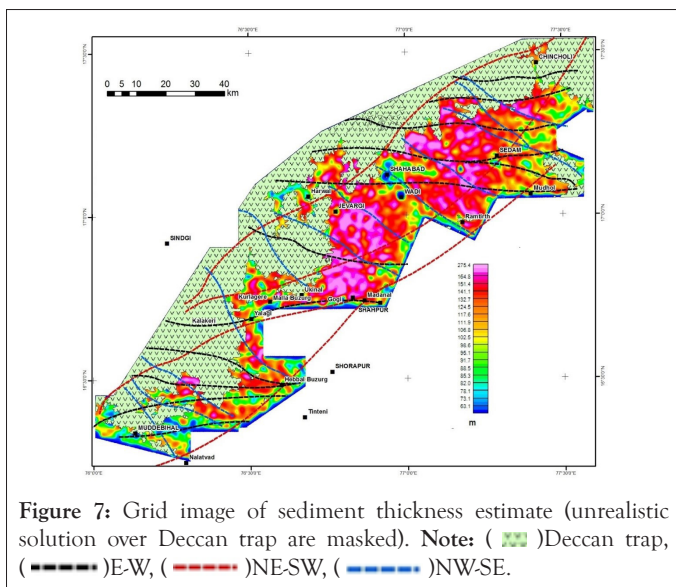


**Figure 7:** Grid image of sediment thickness estimate (unrealistic solution over Deccan trap are masked). **Note:** ( ) Deccan trap, ( ) E-W, ( ) NE-SW, ( ) NW-SE.

## DISCUSSION

### Discussion based on magnetic inferences

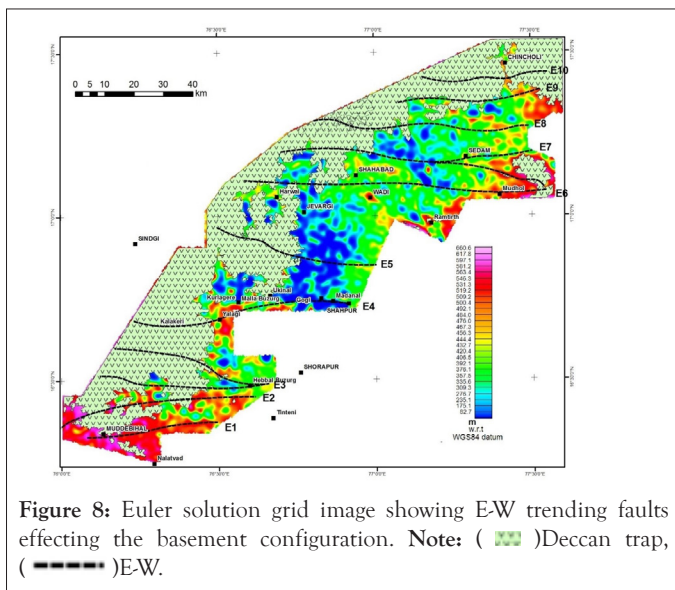
About 2500 m.y. ago the Dharwar craton attained a degree of rigidity *viz.* cratonisation [34], and the platformal sediments in the northern fringe, represented by Kaladgi-Bhima basins overlie a denuded basement comprising Archaean granitoid-greenstone belts and are believed to be spatially interconnected. Kale et al. [35], equated Bhima group with Badami group as they share similar characters *viz.*, lack of significant deformation, the unmetamorphosed nature, and horizontal disposition of the sediment. Brahmam et al. [36], based on regional gravity data suggested that the deposition of the Kaladgi and Bhima sediments in two rift valleys (Koyna and Kurdwadi Rifts) are marked by two conspicuous gravity lows. Temporally, possible age spans of the two basins approximately correspond to the 'boring billion' or 'barren billion' (1.8–0.8 Ga) marked by relative quiescence in plate tectonic movements [37]. Dongre et al. [38], suggested older than 1100 Ma age for Bhima and Kurnool basins from the presence of Bhima and/or Kurnool limestone xenolith within the Siddanpalli Kimberlite (1090 Ma age). The TIMS U-Pb date of  $1266 \pm 76$  Ma for coffinite from the Gogi hydrothermal uranium deposit in the brecciated Shabad Limestones [39], supplement the inference of Bhima deposition prior to 1200 Ma. In view of these aspects, it is prudent to relate tectonic evolution of both Kaladgi-Badami and Bhima basins, contrary to the prevailing hypothesis of evolution of Bhima basin in isolation. Due to lack of comprehensive geophysical data detailed study of Kaladgi and Bhima basins could not be studied particularly their geodynamics, basin geometry and depositional tectonics.

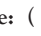

The Kaladgi and Bhima basins encompassed by Peninsular Gneisses, granitoids, and schist belts of Dharwar craton, without any adjoining mobile belt, signify them as intracratonic basins. Typically, intracratonic basins are generally underlain by failed or fossil rifts [40], and sedimentation in rift zones is generally associated with volcanism generated by crustal thinning, mantle upwelling, decompression and consequent partial melting [41]. Magmatism in the form of basic sills are recorded within the lower units of Badami Group around Suldhal area [11], and presence of intrusive bodies concealed beneath the Badami Group of sediments around Islampur area is inferred from the magnetic data [14]. Intra-plate sedimentary basins can be formed in a variety of tectonic settings, including pure extension, transtension, pure strike-slip or compression and are relatively common in continental areas. The initiation of basin development/rifting may be associated with re-activation of pre-existing lineaments or zones of weakness in the crust [42]. van Wees et al. [43], suggested that the geometry of the preexisting fractures and the depth of intracratonic rifts are related. They may develop in two ways: (i) Along preferred fault directions, in which case subsidence areas are limited by rift shoulders, therefore showing sharp thickness changes in their sedimentary fillings along transects perpendicular to the rift axis; or (ii) diffuse borders extending over wide areas [44].

The interpreted linears and major trends from the magnetic data over Bhima basin indicate three major sets i) NW-SE ii) E-W and iii) NE-SW direction, in order of prevalence. The upward continued magnetic image depicting the regional features suggests that the NW-SE and E-W trending features are deep rooted which is corroborated by the Euler solution indicating the NW-SE and E-W trending magnetic features are associated with depth solution exceeding 500 m (Figures 4 and 5). The major trends in the E-W features manifested as nine regional fault signature (marked as E1 to E10). The linear magnetic anomalies along the fault are more consistent with shallower as well as deeper depths and are likely to reflect the position of the edges of the horsts or tilted blocks within the basin, such kind of patterns are recognized in other extensional basin settings [11,45]. Further, the depth to magnetic basement suggests that the block north of the fault is down thrown with respect to the block in the south. Such signatures are prominent in E1 (Tirth Fault), E2 (Hunsagi Fault), E4 (Gogi Fault), E5, E6 (Shahabad Fault), and E7 (Kirni Fault) and E9; however at E3, E8 and E10 the signature shows no such change (Figure 8). The evolution of the Kaladgi-Badami Basin was controlled by movements along east-west trending normal faults under an extensional stress regime [5,37]. The E-W trending features in the southern part of Bhima basin are spatially correlatable with the Jamkhandi Fault and Almatii Fault along the northern basin margin of Kaladgi basin [11]. These faults have affected the Bagalkot Group and probably they are preexisting or reactivated post Bagalkot. It is surmised that this E-W event is responsible for the initial faulting (gravity) with initiation of sedimentation of Badami group basin concomitantly Bhima group.

The signatures for the extensional tectonic are generally not well developed and it is relatively difficult to reconstruct the tectonic evolution of basins, particularly when affected by a strong deformation associated with the subsequent compressional tectonics [45,11]. Relatively low count of NE-SW trending magnetic linears are observed over the Bhima basin which

suggests that either the deformation is limited in nature or the trend are obliterated by later episode. The NE-SW major trends show an anastomosing pattern, which are usually associated with strike-slip fault system and resulting in an en-echelon lozenge shaped depiction [46]. As observed the NE-SW major trends lie along the peripheral part of the Bhima basin, inking as bounding the margins of the basin (Figure 4). The Euler solutions associated with these faults suggest shallow nature (less than 500 m) for these fault zones. At places they seem to have modified/rotated the preexisting E-W faults, as evident conspicuously along Gogi fault. Previously, the Gogi fault was mapped from Gogi to Kurlageri based on the available data and ground observations, however the magnetic data indicate that around Malla buzurg, a NE-SW trending fault affects the Gogi fault and swerves it towards Southwest Kalakeri (inset in Figure 2).



**Figure 8:** Euler solution grid image showing E-W trending faults effecting the basement configuration. Note: (  ) Deccan trap, (  ) E-W.

The most dominant trend observed in the magnetic data is the NW-SE direction, and is seen to have disturbed the precedent trends. These trends indicate to be the most pervasive deformation, and upward continued (1000 m) magnetic image, show the NW-SE signature persists, implying their deep seated nature. The Euler solution indicates deep sources are associated with the NW-SE trends and corroborate the inference of deep seated nature of the fault. These NW-SE trending features have major role in defining the present day basin configuration. The most prominent of these faults is the Wadi fault, and the Euler solutions associated with this fault suggest it as a deep seated fault. The sediment thickness image indicate thicker succession lying NE of the Wadi fault, further suggesting that the northern block of the NW-SE trending fault is thrown down (Figure 7). The NW-SE faults indicate displacement both in strike and dip and have dislocated the precursor E-W and NE-SW faults. Rajaram et al. [47], suggested that the NW-SE magnetic trends around the northern part of Dharwar craton are also seen within the Bastar craton and are in accordance with the Godavari Graben trends and may have been influenced by the opening of the Godavari Graben. The greenstone belts of the EDC viz., Mangalur, Raichur and Narayanpet have regional trends along NNW-SSE to NW-SE which is nearly perpendicular the long axis of the oval shaped Bhima basin, it would be a construe to imply NW-SE trends in basin evolution.

The inlier exposed around Shahabad lie between the E-W

faults E6 and E7; occur at the intersection of Wadi fault. The shallow basement and the inlier are possibly the manifestation of the faults, and might have resulted by rotation fault (scissor-faults, which change from a normal fault at one end to a reverse fault at the other). This inference supports the thicker sediment sequence on the north down thrown block of the Wadi fault and a shallow/exposed basement to the South.

### Discussion and its implication on basin evolution

The evolution model by Jayaprakash et al. [5], proposes the NE-SW transtensional fault systems, with secondary and tertiary shears developed along initial planes of weakness, all in unison to form lozenge shaped graben thus initiating the Bhima basin. Jayaprakash et al. [5], opined that middle Proterozoic Eastern Ghat Mobile Belt (EGMB) orogenic event (around 1.0 Ga) involving the subduction of the eastern margins of the Dharwar Protocontinents gave rise to transtensional faults, which are responsible for extension and yielded pull apart basins. This hypotheses presumed the evolution of Bhima basin in Neoproterozoic times, and the new geochronological data suggest revision of age of Bhima basin into the Mesoproterozoic (~1.1-1.2 Ga) [38,39]. The EGMB is the product of the collision between East Antarctica and India [48]. Recent reliable geochronology, geothermometric and geobarometric studies of EGMB rock units indicate that the docking between the two continents did not occur until about 1.1 Ga and continued up to 0.55 Ga, roughly coinciding with the Rodinia assembly [49,50]. In view of these geochronological data, it is evident that the sedimentation of Bhima basin occurred prior to the exhumation of the EGMB. The NE-SW faults associated with Bhima basin development may be a reactivation of structures that are parallel to the passive margin prior to the collision with East Antarctica. Invoking the compressive forces involving 1.0 Ga EGMB orogenic event with left lateral strike slip for initiation of NE-SW lozenge shaped Bhima basin lying as close as 200 km can be ruled out. Further, the NW-SE and the NE-SW trending faults have affected the E-W trending faults as suggested by the magnetic data. The kinematic evolution proposed by Jayaprakash et al. [5], of riedel shears, which are subsidiary shear fractures that propagate a short distance out of the main fault are synchronous movement on all fractures accommodate strain in the fault zone i.e. coeval with NE-SW main fault, is untenable.

Kale et al. [4], have opined that a shear couple along NW-SE with dextral transtensional movement has resulted in the form of a shallow pull-apart basin. Further, added that this movement resulted in east-west-trending second-order gravity faults, giving rise to rectilinear sags filled up with shallow water sediments. However, the magnetic data indicate that the E-W trends are regional trends and are disturbed by NW-SE direction faults. It is inferred from this study that a compression from SE, has resulted in dextral displacement along the Wadi fault, being the main axis and has affected the preexisting E-W faults, particularly evident in Gogi fault. The dip of major faults limiting the basin also influences the relative position of the fault walls with respect to their previous role during extension [51]. That is, the dip of faults defines whether the downthrown block during the extensional stage will become uplifted or remain downthrown during inversion. Steeply dipping faults can be a catalyst for the relative position of the two blocks to remain unchanged and for folding and thrusting processes to affect the main fault. This

one may change its dip sense to finally become a reverse fault. In the E-W trending Gogi fault, the reverse faulting is observed in segments only and not along the entire length of the fault and has probably originated due to compression from southeastern direction [52]. Due to overriding process during reverse faulting the beds of limestone got folded and forms steep southerly dip with fault breccia. Post depositional hydrothermal uranium and copper mineralization occur along a few east-west-trending faults, which extend into the basement granitoids *viz.*, Gogi-Kurlagere Fault zone. As evident at Gogi uranium deposit, the basement granitoid is uplifted over the Bhima sediments [53]. This suggests that movement along some faults occurred in the post-depositional period also, as manifested in Bhima sediments which are gently dipping to steep dips along the E-W and NW-SE trending basin margins faults. Exceptionally, at places the NE-SW trends are seen dislocated by E-W trends, considering the above facts it can be assumed that during compression along SE direction, the reactivation of E-W trends might have yielded it. The qualitative and quantitative analysis of the magnetic data, suggest that the E-W trending faults are normal faults and generally the northern block is down thrown. These faults are later effected by NE-SW trending shear couple, in its entirety resulting in shallow depression bounded by NE-SW, where sedimentations have taken place and the NW-SE trending faults seems to the reactivation of inherent structural grain of Dharwar Craton [54,55]. The sedimentation of Bhima basin represent platform deposits of shallow marine, near shore environments and is indisputably concluded by sedimentological studies [2,4,5].

## CONCLUSION

With the comprehensive coverage of high resolution airborne magnetic data over Bhima basin, withal the inferences are drawn *viz.*, the E-W, NE-SW and NW-SE faults their disposition, basement configuration and estimation of thickness of sediment pile and further suggests that the Bhima basin has possibly evolved over a failed E-W trending rift zone, surmised as reactivation in the northern Dharwar Craton, after sedimentation of Bagalkot group. Later the NE-SW shear couple bounding the geometry to a lozenge shape with long axis along NE-SW, probably defines the basin boundaries, can be correlated with the docking of EGMB. The last episode is the NW-SE trending dextral strike slip faults which has affected the Bhima sediments as well as the preceding E-W and NE-SW trends, have defined the present day basin configuration.

## REFERENCES

- Chakraborty PP, Dey S, Mohanty SP. Proterozoic platform sequences of Peninsular India: Implications towards basin evolution and supercontinent assembly. *J Asian Earth Sci.* 2010;39(6):589-607.
- Akhtar K. Depositional environment, dispersal pattern and paleogeography of the clastic sequence in the Bhima basin. *Indian Mineral.* 1977;18:65-72.
- Kale VS, Peshwa VV. A Proterozoic pull-apart basin: Interpretation based on remotely sensed data. In 28th Geological Congress Washington. 1989;2:149-150.
- Kale VS, Peshwa VV. Bhima Basin. Geological Society of India, Bangalore. 1995.
- Jayaprakash AV. Purana basins of Karnataka. Geological Survey of India. 2007:129.
- Mudholkar AV, Peshwa VV. Clastic limestone dikes from the late Proterozoic Bhima group, South India. *Sediment Geol.* 1988;57(3-4):221-219.
- Ananthanarayana H, Abbas MH. GSI Report. 1987.
- Ramakrishna TS, Chayanulu AY. A geophysical appraisal of the Purana basins of India. *Geol Soc India.* 1988;32(1):48-60.
- McLean MA, Wilson CJ, Boger SD, Betts PG, Rawling TJ, Damaske D. Basement interpretations from airborne magnetic and gravity data over the Lambert Rift region of East Antarctica. *J Geophys Res: Solid Earth.* 2009;114(B6).
- Stewart JR, Betts PG. Late Paleo-Mesoproterozoic plate margin deformation in the southern Gawler Craton: Insights from structural and aeromagnetic analysis. *Precambrian Res.* 2010;177(1-2):55-72.
- Sridhar M, Babu VR, Markandeyulu A, Raju BV, Chaturvedi AK, Roy MK. A reassessment of the Archean-Mesoproterozoic tectonic development of the southeastern Chhattisgarh Basin, Central India through detailed aeromagnetic analysis. *Tectonophysics.* 2017;712:289-302.
- Nabighian MN, Grauch VJ, Hansen RO, LaFehr TR, Li Y, Peirce JW, et al. The historical development of the magnetic method in exploration. *Geophysics.* 2005;70(6):33-61.
- Aitken AR, Betts PG. Multi-scale integrated structural and aeromagnetic analysis to guide tectonic models: An example from the eastern Musgrave Province, Central Australia. *Tectonophysics.* 2009;476(3-4):418-435.
- Sridhar M, Markandeyulu A, Chawla AS, Chaturvedi AK. Analyses of aeromagnetic data to delineate basement structures and reveal buried igneous bodies in Kaladgi Basin, Karnataka. *J Geol Soc India.* 2018;91:165-173.
- Gunn PJ. Application of aeromagnetic surveys to sedimentary basin studies. *AGSO J Australian Geol Geophys.* 1997;17:133-144.
- Foss CA, Shi ZS, Teasdale J, Pryer LL, Loutit TS, Stuart-Smith PG, et al. Interpretation of basin structure from high resolution aeromagnetic data: An example from the officer Basin of South Australia. In PESA Eastern Australasian Basins Symposium II. 2004:257-264.
- Grauch VJ, Connell SD, Hudson MR. New perspectives on the geometry of the Albuquerque Basin, Rio Grande rift, New Mexico: Insights from geophysical models of rift-fill thickness. In *New Perspectives on Rio Grande Rift Basins: From Tectonics to Groundwater: Geological Society of America Special Paper.* 2013;494:427-462.
- Drenth BJ, Grauch VJ, Ruleman CA, Schenk JA. Geophysical expression of buried range-front embayment structure: Great Sand Dunes National Park, Rio Grande rift, Colorado. *Geosphere.* 2017;13(3):974-990.
- Chadwick B, Vasudev VN, Hegde GV. The Dharwar craton, southern India, interpreted as the result of Late Archaean oblique convergence. *Precambrian Res.* 2000;99(1-2):91-111.



20. Naqvi SM. Geology and Evolution of the Indian Plate. 2005:450.
21. Naqvi SM, Rogers JJ. Precambrian geology of India. Oxford University Press. 1987:223.
22. Ramakrishnan M, Vaidyanadhan R. Geology of India. Geol Soc India. 2008;1:994.
23. Peshwa V, Chitrao A. Status of the Metamorphics-Bhima sediments boundary: A study based on remote sensing techniques. In Proceedings of 4th Asian Conference Remote Sensing, Colombo, Sri Lanka Q-11-1-Q-11-9. 1983.
24. Mishra RN, Jayaprakash AV, Hans SK, Sundaram V. Bhima group of upper Proterozoic-a stratigraphic puzzle. Mem Geol Soc India. 1987;6:227-237.
25. Dunne WM, Hancock PL. Palaeostress analysis of small-scale brittle structures. In Continental deformation 1994:101-120.
26. Swain CJ. A FORTRAN IV program for interpolating irregularly spaced data using the difference equations for minimum curvature. Comput Geosci. 1976;1(4):231-240.
27. Rajagopalan S. Analytic signal vs. reduction to pole: Solutions for low magnetic latitudes. Explor Geophys. 2003;34(4):257-262.
28. Grant FS. Aeromagnetism, geology and ore environments, I. Magnetite in igneous, sedimentary and metamorphic rocks: An overview. Geoexploration. 1985;23(3):303-333.
29. Miller HG, Singh V. Potential field tilt-a new concept for location of potential field sources. J Appl Geophys. 1994;32(2-3):213-217.
30. Babu VR, Patra I, Tripathi S, Raju BV, Chaturvedi AK. High resolution airborne magnetic data-an aid to delineate favorable basement structures for uranium exploration in parts of Palnad and Srisailem sub-basins, Cuddapah Basin, India. India Explor Res Atom Min. 2012;22:141-152.
31. Reid AB, Allsop JM, Granser H, Millett AT, Somerton IW. Magnetic interpretation in three dimensions using Euler deconvolution. Geophysics. 1990;55(1):80-91.
32. Mushayandebvu MF, van Driel P, Reid AB, Fairhead JD. Magnetic source parameters of two-dimensional structures using extended Euler deconvolution. Geophysics. 2001;66(3):814-823.
33. Ku CC, Sharp JA. Werner deconvolution for automated magnetic interpretation and its refinement using Marquardt's inverse modelling. Geophysics. 1983;48(6):754-774.
34. Radhakrishna BP, Vaidyanathan R. Geology of Karnataka. Geological Society of India, Bangalore. 1997.
35. Kale VS, Phansalkar VG. Purana basins of peninsular India: A review. Basin Res. 1991;3(1):1-36.
36. Brahmam NK, Negi JG. Rift valleys beneath Deccan traps (India). Geophys Res Bull. 1973;11(3):207-237.
37. Dey S. Geological history of the Kaladgi-Badami and Bhima basins, south India: Sedimentation in a Proterozoic intracratonic setup. In Precambrian Basins of India: Stratigraphic and Tectonic Context. 2015;43:283.
38. Dongre A, Rao NVC, Kamde G. Limestone xenolith in Siddanpalli Kimberlite, Gadwal granite-greenstone terrain, eastern Dharwar craton, Southern India: Remnant of Proterozoic platformal cover sequence of Bhima/Kurnool Age?. J Geol. 2008;116(2):184-191.
39. Pandey BK, Natarajan V, Krishna V, Pandit SA. U-Pb and Sm-Nd isotopic studies on uraniumiferous brecciated limestone from Bhima basin: Evidence for a Mesoproterozoic U-mineralization event in Southern Peninsular India. In Significant milestones in the growth of geochemistry in India during the 50 year Period:1958-2008. 2008.
40. Klein G. Intracratonic basins. In Tectonics of sedimentary basins. 1995:459-478.
41. Allen PA, Allen JR. Basin analysis: Principles and application to petroleum play assessment. John Wiley and Sons; 2013.
42. Miall AD. Principles of sedimentary basin analysis. Springer Science and Business Media. 2013.
43. van Wees JD, Arche A, Bejedorff CG, López-Gómez J, Cloetingh SA. Temporal and spatial variations in tectonic subsidence in the Iberian Basin (eastern Spain): Inferences from automated forward modelling of high-resolution stratigraphy (Permian-Mesozoic). Tectonophysics. 1998;300(1-4):285-310.
44. Sopeña A, Sánchez-Moya Y. Tectonic systems tract and depositional architecture of the western border of the Triassic Iberian Trough (central Spain). Sediment Geol. 1997;113(3-4):245-267.
45. Betts PG, Giles D, Lister GS. Aeromagnetic patterns of half-graben and basin inversion: Implications for sediment-hosted massive sulfide Pb-Zn-Ag exploration. J Struct Geol. 2004;26(6-7):1137-1156.
46. Mann P, Hempton MR, Bradley DC, Burke K. Development of pull-apart basins. J Geol. 1983;91(5):529-554.
47. Rajaram M, Anand SP. Aeromagnetic signatures of Precambrian shield and suture zones of Peninsular India. Geosci Front. 2014;5(1):3-15.
48. Rogers JJ. The Dharwar craton and the assembly of peninsular India. J Geol. 1986;94(2):129-143.
49. Kumar KV, Leelanandam C. Evolution of the Eastern Ghats Belt, India: A plate tectonic perspective. Geol Soc India. 2008;72(6):720-749.
50. Veevers JJ. Palinspastic (pre-rift and-drift) fit of India and conjugate Antarctica and geological connections across the suture. Gondwana Res. 2009;16(1):90-108.
51. Soto R, Casas-Sainz AM, Del Rio P. Geometry of half-grabens containing a mid-level viscous décollement. Basin Res. 2007;19(3):437-450.
52. Roy D, Bhattacharya D, Mohanty R, Patnaik S, Pradhan AK, Chakrabarti K, et al. Deformation pattern in Gogi-Kurlagere fault zone at Gogi-Kanchankayi sector of Proterozoic Bhima Basin of northern Karnataka: Implication in control of uranium mineralization. Expl Res Atom Min. 2016;26:157-176.

53. Chaki A, Pannerselvam A, Chavan SJ. Uranium exploration in the Upper Proterozoic Bhima basin, Karnataka, India: A new target area. In: Uranium Production and Raw Materials for the Nuclear Fuel Cycle—Supply and Demand, Economics, the Environment and Energy Security. International Atomic Energy Agency, Vienna, Proceedings Series. 2005:183-194.
54. Kale VS. Constraints on the evolution of the Purana basins of peninsular India. *J Geol Soc India*. 1991;38(3):231-252.
55. Singh IB. Precambrian sedimentary sequences of India: Their peculiarities and comparison with modern sediments. *Precambrian Res*. 1980;12(1-4):411-436.